

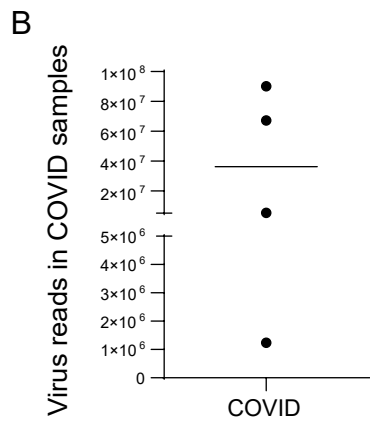
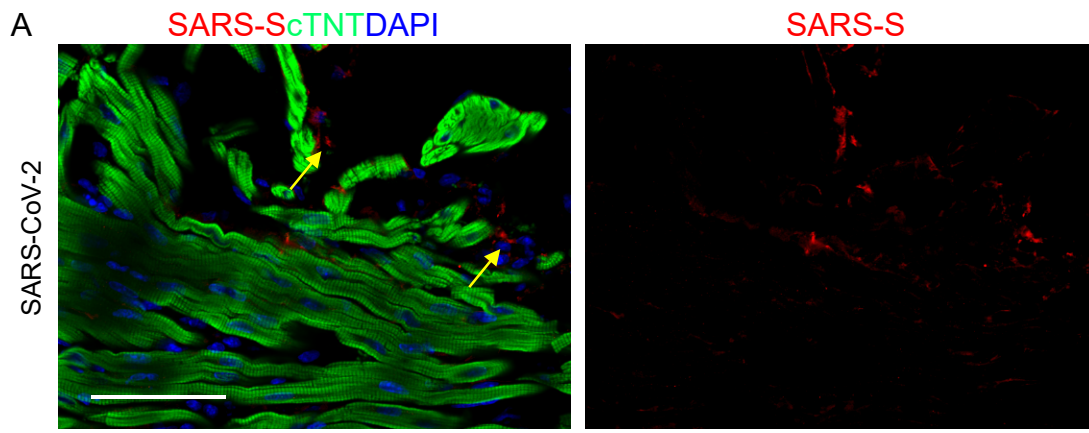
Supplemental Information

Cardiomyocytes recruit monocytes upon SARS-CoV-2 infection by secreting CCL2

Liulu Yang, Benjamin E. Nilsson-Payant, Yuling Han, Fabrice Jaffré, Jiajun Zhu, Pengfei Wang, Tuo Zhang, David Redmond, Sean Houghton, Rasmus Møller, Daisy Hoagland, Lucia Carrau, Shu Horiuchi, Marisa Goff, Jean K. Lim, Yaron Bram, Chanel Richardson, Vasuretha Chandar, Alain Borczuk, Yaoxing Huang, Jenny Xiang, David D. Ho, Robert E. Schwartz, Benjamin R. tenOever, Todd Evans, and Shuibing Chen

SUPPLEMENTAL INFORMATION

Figure S1



Supplemental Figure Legends

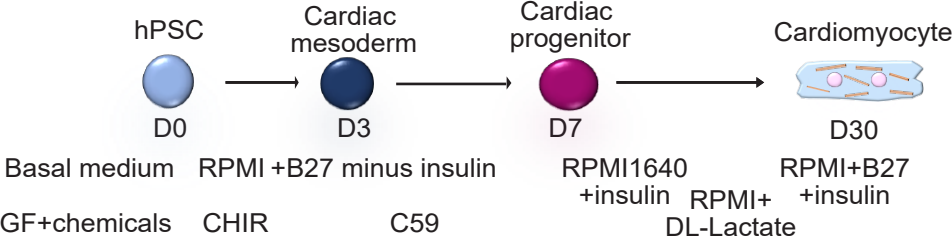
Figure S1. SARS-S staining in infected hamster heart tissue and viral reads in human COVID-19 heart samples, related to Figure 1.

(A) Immunofluorescences staining shows and example of SARS-S signal in non-CMs. Scale bar=50 μm .

(B) Total virus RNA-seq reads in human COVID-19 samples (N=4 COVID-19 patients).

Figure S2

A



B

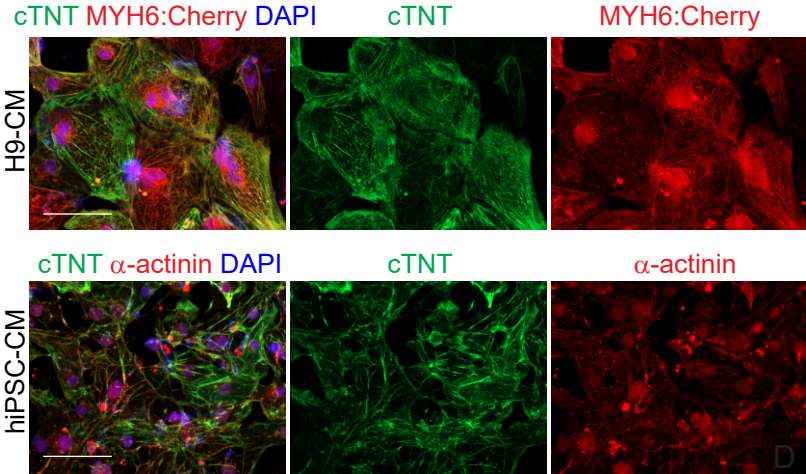


Figure S2. Stepwise differentiation of hPSCs toward CMs, related to Figure 3.

(A) Scheme of stepwise differentiation of hPSCs toward CMs.

(B) Immunostaining of the hPSC-derived CMs. Scale bar= 100 μm .

Figure S3

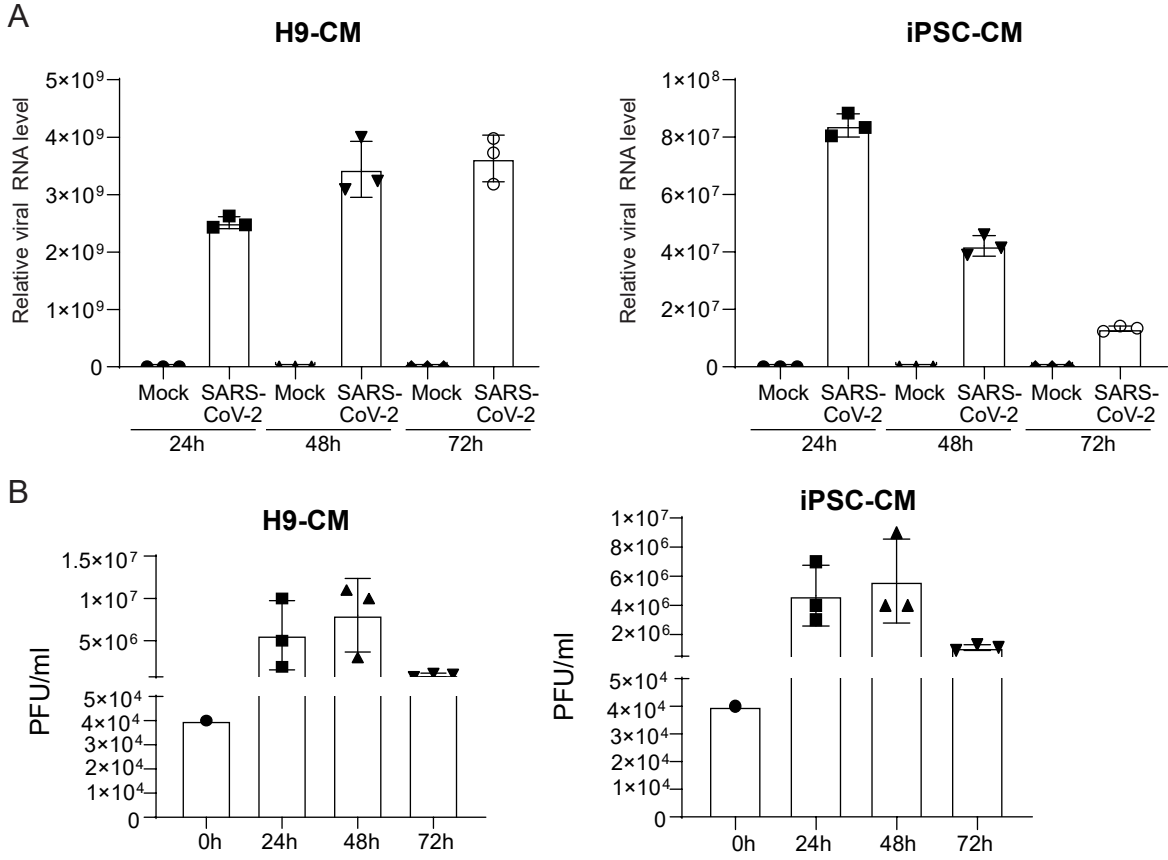


Figure S3. Time course experiment to monitor the SARS-CoV-2 infection on hESC-derived and iPSC-derived CMs, related to Figure 3.

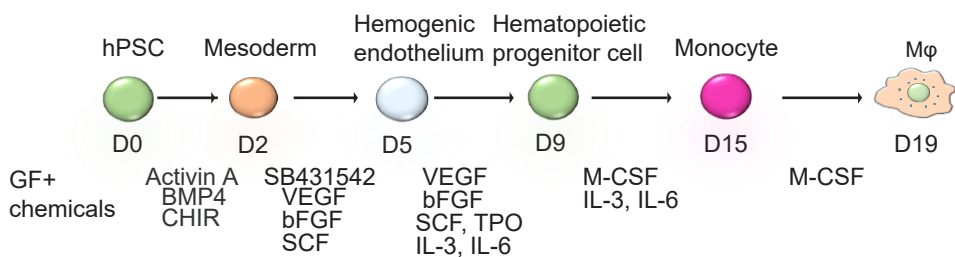
(A) Relative viral RNA expression levels in mock or SARS-CoV-2 (MOI=0.1) infected H9-derived CMs or iPSC-derived CMs at 24, 48, 72 hpi.

(B) Plaque assay of mock or SARS-CoV-2 (MOI=0.1) infected H9-derived CMs or iPSC-derived CMs at 0, 24, 48, 72 hpi. Red lines indicate the input virus (0h indicates the input virus: 4×10^4 Pfu).

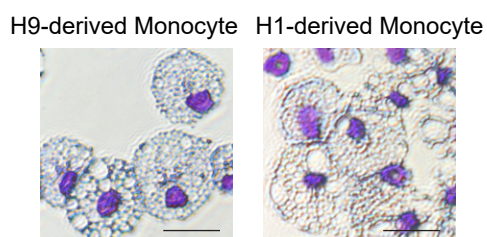
N=3 independent biological replicates. Data was presented as mean \pm STDEV.

Figure S4

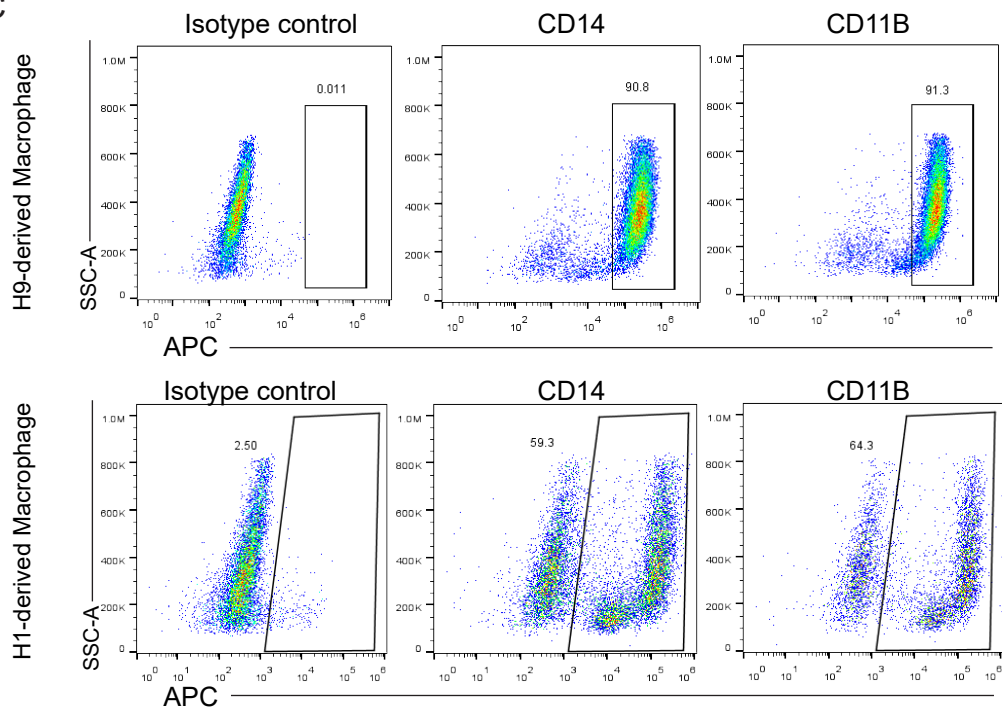
A



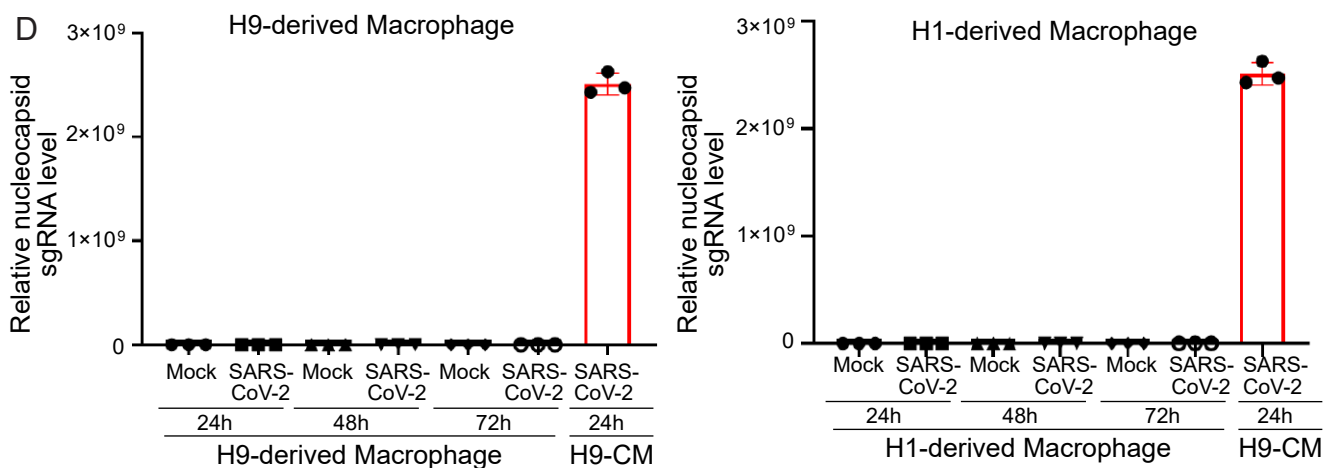
B



C



D



E

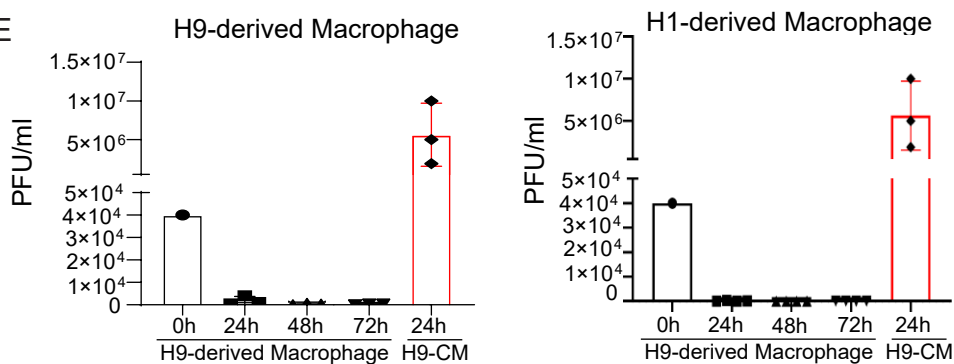


Figure S4. Stepwise differentiation of hPSCs toward macrophages, related to Figure 6.

- (A) Scheme of stepwise differentiation of hPSCs toward macrophages.
- (B) Swiss-Giemsa staining of hPSC-derived monocytes. Scale bar= 25 μ m.
- (C) FACS analysis of hPSC-derived macrophages using CD14 and CD11B antibodies.
- (D) Relative viral RNA expression levels in mock or SARS-CoV-2 (MOI=0.1) infected H9-derived macrophages or H1-derived macrophages at 24, 48, 72 hpi. Relative viral RNA expression in SARS-CoV-2 infected CMs at 24 hpi was included as a positive control.
- (E) Plaque assay of mock or SARS-CoV-2 (MOI=0.1) infected H9-derived macrophages or H1-derived macrophages at 0, 24, 48, 72 hpi. Plaque numbers of SARS-CoV-2 infected CMs at 24 hpi was included as a positive control. (0h indicates the input virus: 4×10^4 Pfu).

N=3 independent biological replicates. Data was presented as mean \pm STDEV.

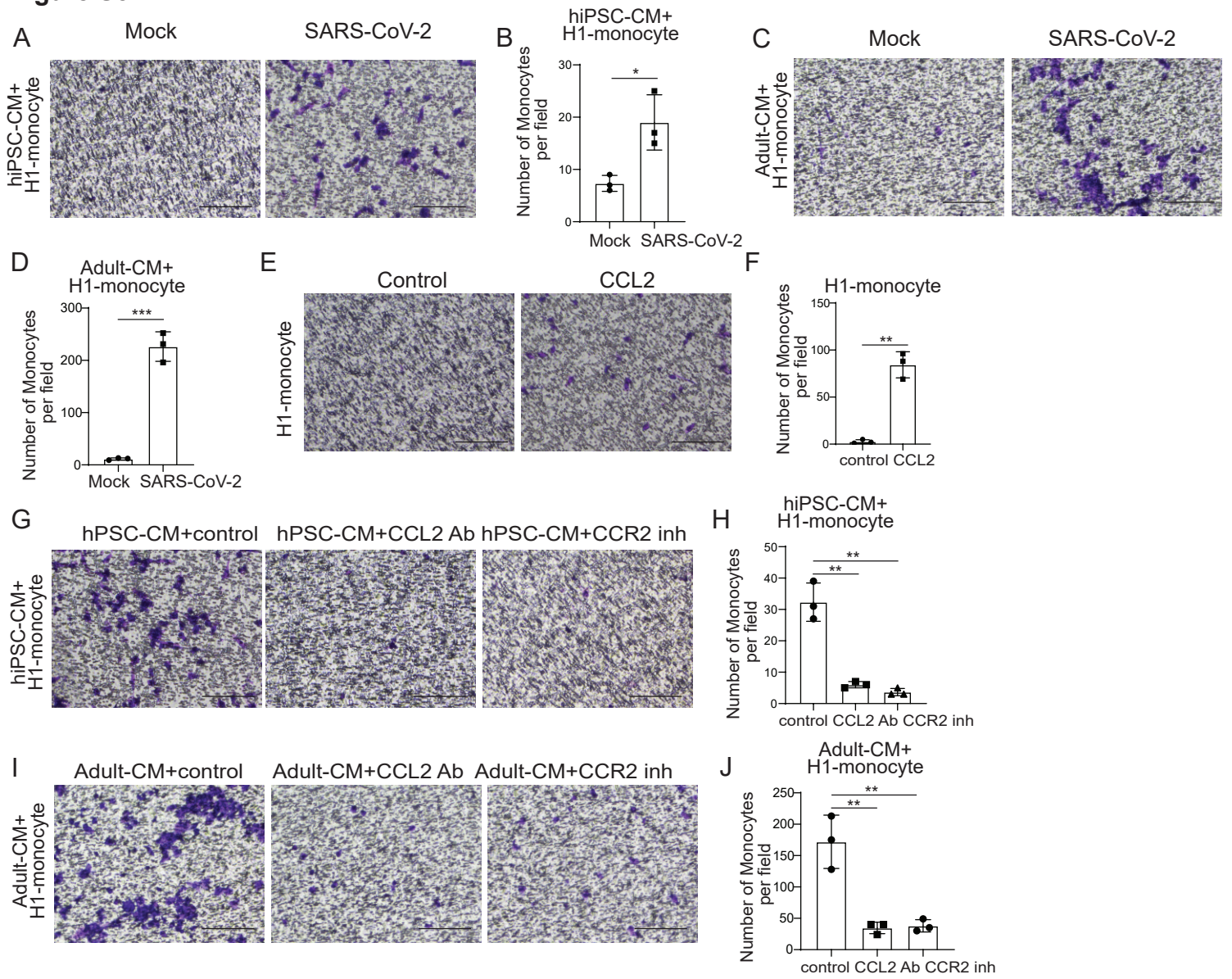
Figure S5

Figure S5. CMs recruit monocytes following SARS-CoV-2 infection through secreting CCL2, related to Figure 6.

(A and B) Phase contrast images (A) and quantification (B) of migrated H1-derived monocytes recruited by hiPSC-derived CMs infected with SARS-CoV-2 virus or mock-infected in the monocyte migration assay. Scale bar= 100 μ m.

(C and D) Phase contrast images (C) and quantification (D) of H1-derived monocytes recruited by adult human CMs infected with SARS-CoV-2 virus or mock-infected in the monocyte recruitment assay. Scale bar= 100 μ m.

(E and F) Phase contrast images (E) and quantification (F) of migrated H1-derived monocytes by CCL2 in the monocyte recruitment assay. Scale bar= 100 μ m.

(G and H) Phase contrast images (G) and quantification (H) of migrated H1-derived monocytes recruited by hiPSC-derived CMs infected with SARS-CoV-2 virus and treated with CCL2 neutralizing antibody or CCR2 inhibitor (RS504393) in the monocyte recruitment assay. Scale bar= 100 μ m.

(I and J) Phase contrast images (I) and quantification (J) of migrated H1-derived monocytes recruited by adult human CMs infected with SARS-CoV-2 virus and treated with CCL2 neutralizing antibody or CCR2 inhibitor in the monocyte recruitment assay. Scale bar= 100 μ m.

N=3 independent biological replicates. Data was presented as mean \pm STDEV. *P* values were calculated by unpaired two-tailed Student's *t* test. **P* < 0.05, ***P* < 0.01, and ****P* < 0.001.

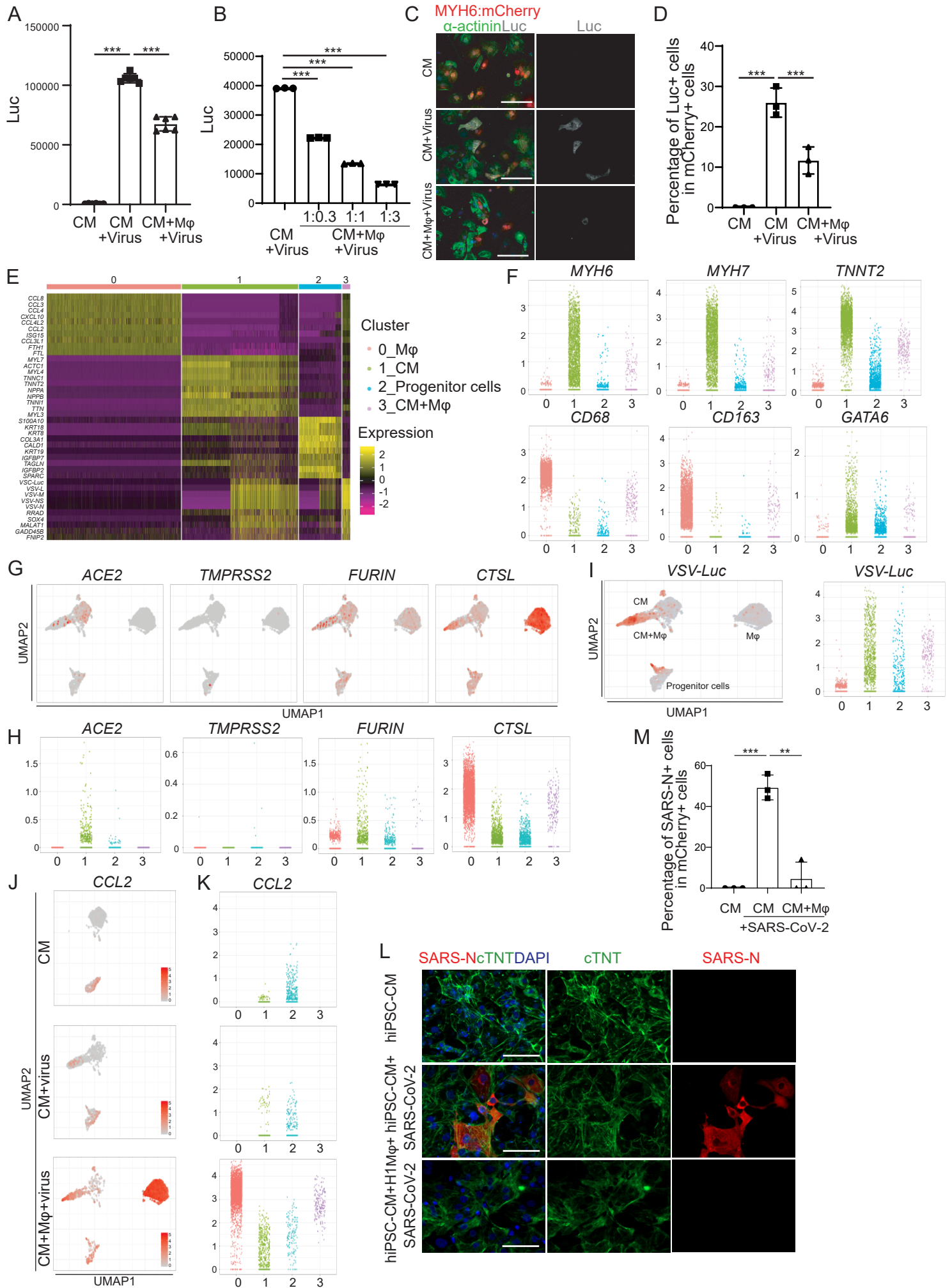
Figure S6

Figure S6. Single cell RNA-seq analysis of immunocardiac co-cultured cells upon SARS-CoV-2-entry virus infection, related to Figure 7.

(A) Luciferase activity at 24 hpi of hPSC-derived CMs mock-infected or infected with SARS-CoV-2-entry virus in the presence or absence of macrophages (MOI=0.1).

(B) Luciferase activity at 24 hpi of H9-derived CMs infected with SARS-CoV-2-entry virus and co-cultured with different ratio of macrophages (MOI=0.1).

(C and D) Immunostaining **(C)** and quantification **(D)** of Luc in hPSC-derived CMs at 24 hpi mock-infected or infected with SARS-CoV-2-entry virus in the presence or absence of macrophages (MOI=0.1).

(E) Heatmap of enriched genes in each cluster of scRNA profiles of the immunocardiac co-culture platform containing hPSC-derived CMs and macrophages upon SARS-CoV-2-entry virus infection.

(F) Jitter plot of cell type specific markers in the immunocardiac co-culture platform containing hPSC-derived CMs and macrophages upon SARS-CoV-2-entry virus infection.

(G) UMAP of *ACE2*, *TMPRSS2*, *FURIN*, *CTSL* genes in the immunocardiac co-culture platform containing H9-derived CMs and macrophages upon SARS-CoV-2-entry virus infection.

(H) Jitter plot of *ACE2*, *TMPRSS2*, *FURIN*, *CTSL* genes in the immunocardiac co-culture platform containing H9-derived CMs and macrophages upon SARS-CoV-2-entry virus infection.

(I) UMAP and jitter plot of SARS-CoV-2-entry virus gene in the immunocardiac co-culture platform containing hPSC-derived CMs and macrophages upon SARS-CoV-2-entry virus infection.

(J) UMAP analysis of *CCL2* in H9-derived CMs mock-infected (CM) or infected with SARS-CoV-2-entry virus (CM+virus) and the virus-immunocardiac co-culture platform containing H9-derived CMs and H9-derived macrophages infected with SARS-CoV-2-entry virus (CM+macrophage+virus).

(K) Jitter plot of *CCL2* in H9-derived CMs mock-infected (CM) or infected with SARS-CoV-2-entry virus (CM+virus) and the virus-immunocardiac co-culture platform containing H9-derived CMs and H9-derived macrophages infected with SARS-CoV-2-entry virus (CM+macrophage+virus).

(L and M) Immunostaining **(L)** and quantification **(M)** of SARS-N⁺ cells in cTNT⁺ hiPSC-derived CMs at 24 hpi mock-infected or infected with SARS-CoV-2 in the presence or absence of H1-derived macrophages (MOI=0.1). Scale bar= 50 μ m.

N=3 independent biological replicates. Data was presented as mean \pm STDEV. *P* values were calculated by unpaired two-tailed Student's *t* test. ***P* < 0.01, and ****P* < 0.001.

Figure S7

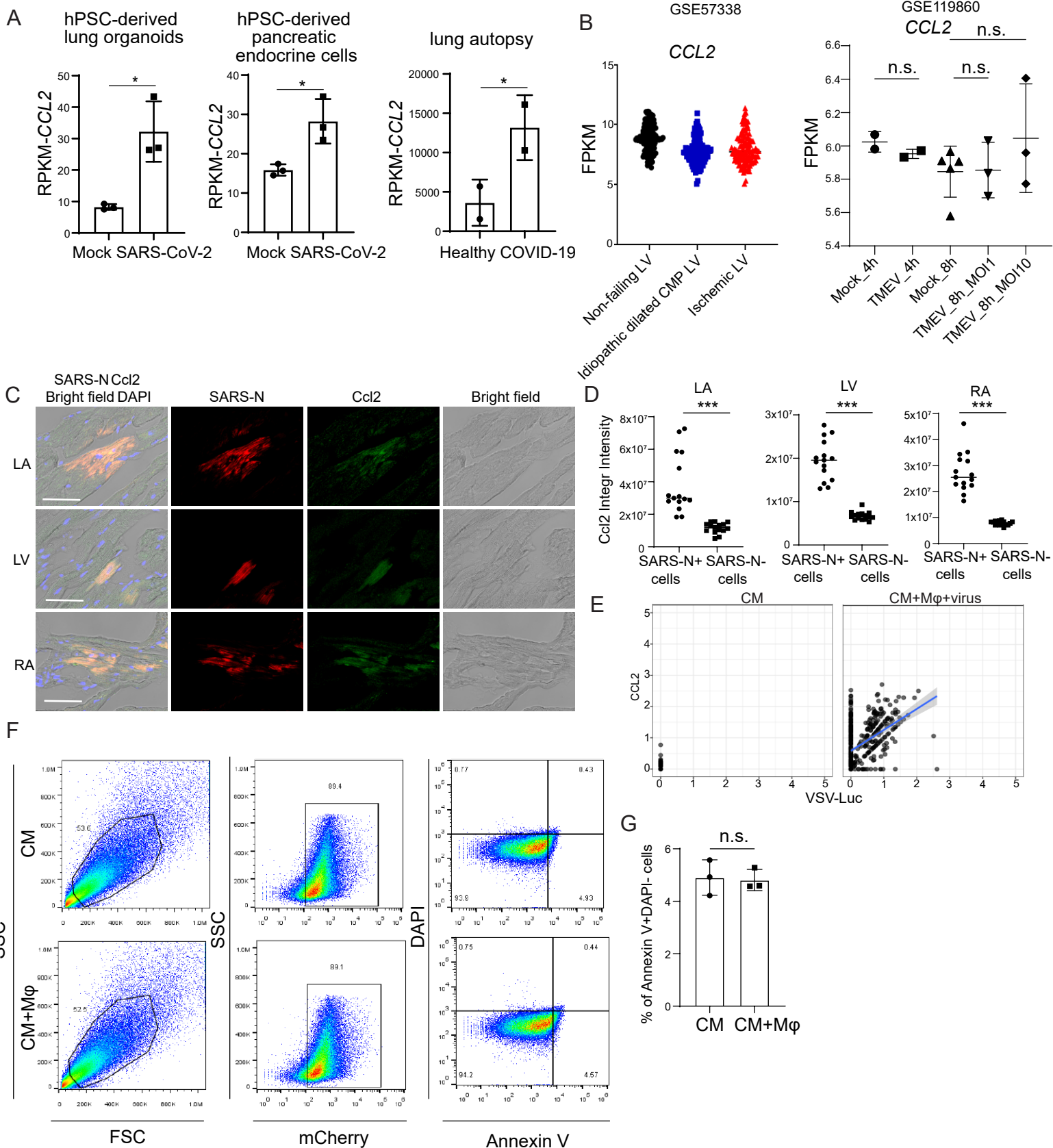


Figure S7. CCL2 expression in SARS-CoV-2 infected cells and COVID-19 patients, related to Figure 7.

(A) *CCL2* expression levels in mock-infected or SARS-CoV-2 infected hPSC-derived lung organoids (N=3 for mock, N=3 for SARS-CoV-2), hPSC-derived pancreatic endocrine cells (N=3 for mock, N=3 for SARS-CoV-2) and lung autopsy samples of non-COVID-19 (N=2) and COVID-19 patients (N=2).

(B) Left, *CCL2* expression of non-failing LVs, idiopathic dilated cardiomyopathy LVs and ischemic LVs (GSE57338). Right, *CCL2* expression in murine encephalomyelitis virus (TMEV) infected cardiomyocytes or mock infected cardiomyocytes (GSE119860).

(C and D) Immunostaining (C) and quantification (D) of SARS-N and Ccl2 in SARS-CoV-2 infected hamster heart. Scale bar = 50 μ m.

(E) Correlation between *CCL2* expression and VSV-Luc expression in CM and CM+macrophage+virus groups.

(F and G) Flow cytometry analysis (F) and quantification (G) of apoptotic cells in H9-derived CMs in the presence or absence of H9-derived macrophages using a trans-well assay.

N=3 independent biological replicates. Data was presented as mean \pm STDEV. *P* values were calculated by unpaired two-tailed Student's *t* test. **P* < 0.05, ****P* < 0.001 and n.s., non-significant.

Movie S1. Ca²⁺ flux intensity of mock infected H9-derived CMs at 48 hpi, related to Figure 3.

Movie S2. Ca²⁺ flux intensity of SARS-CoV-2 infected H9-derived CMs at 48 hpi, related to Figure 3.

Table S1. Antibodies used for immunocytochemistry and intracellular flow cytometric analysis, related to Figure 1, Figure 2, Figure 3, Figure 5 and Figure 7.

Table S2. Primers used for qRT-PCR, related to Figure 3, Figure 5 and Figure 7.

Primer name	Sequence
<i>ACTB</i> -human-Forward	<i>CGTCACCAACTGGGACGACA</i>
<i>ACTB</i> - human-Reverse	<i>CTTCTCGCGGTTGGCCTTGG</i>
<i>SARS-CoV-2-TRS-L</i>	<i>CTCTTGTAGATCTGTTCTCTAAACGAAC</i>
<i>SARS-CoV-2-TRS-N</i>	<i>GGTCCACCAAACGTAATGCG</i>
<i>cTNT</i> -Forward	<i>TTCACCAAAGATCTGCTCCTCGCT</i>
<i>cTNT</i> -Reverse	<i>TTATTACTGGTGTGGAGTGGGTGTGG</i>
<i>ACTB</i> -hamster-Forward	<i>CACCATTGGCAACGAGCGGTTC</i>
<i>ACTB</i> - hamster-Reverse	<i>AGGTCTTTGCGGATGTCGACGT</i>
<i>CCL2</i> -hamster-Forward	<i>CAGCCAGACTCCGTAACTCC</i>
<i>CCL2</i> - hamster-Reverse	<i>TGTATGCCTGGACCCAGTCCT</i>

EXPERIMENTAL PROCEDURES

Cell lines

Vero E6 (African green monkey [*Chlorocebus aethiops*] kidney) were obtained from ATCC (<https://www.atcc.org/>). Cells were cultured in Dulbecco's Modified Eagle Medium (DMEM) supplemented with 10% FBS and 100 I.U./mL penicillin and 100 µg/mL streptomycin. All cell lines were incubated at 37°C with 5% CO₂.

Propagation and titration of SARS-CoV-2

SARS-CoV-2, isolate USA-WA1/2020 (NR-52281) was deposited by the Center for Disease Control and Prevention and obtained through BEI Resources, NIAID, NIH. SARS-CoV-2 was propagated in Vero E6 cells in DMEM supplemented with 2% FBS. Virus stocks were filtered and concentrated by centrifugation using Amicon Ultra-15 Centrifugal filter units (100 KDa MWCO). Infectious titers were determined by plaque assays in Vero E6 cells in Minimum Essential Media supplemented with 2% FBS, 4 mM L-glutamine, 0.2% BSA, 10 mM HEPES and 0.12% NaHCO₃ and 0.7% OXOID agar as has been described previously (Blanco-Melo et al., 2020). All work involving live SARS-CoV-2 was performed in the CDC/USDA-approved BSL-3 facility of the Global Health and Emerging Pathogens Institute at the Icahn School of Medicine at Mount Sinai in accordance with institutional biosafety requirements.

SARS-CoV-2 infections of hamsters

3-5-week-old male Golden Syrian hamsters (*Mesocricetus auratus*) were obtained from Charles River. Hamsters were acclimated to the CDC/USDA-approved BSL-3 facility of the Global Health and Emerging Pathogens Institute at the Icahn School of Medicine at Mount Sinai for 2-4 days. Before intranasal infection, hamsters were anesthetized by intraperitoneal injection with a ketamine HCl/xylazine solution (4:1). Hamsters were intranasally inoculated with 100 pfu of SARS-CoV-2 in PBS (or PBS only as a control) in a total volume of 100 µl. Two days post-infection hamsters were euthanized and hearts were collected. For hearts analyzed by immunofluorescence staining, hamsters were perfused with 60 ml of ice-cold PBS before tissue collection and collected hearts were immediately placed in 10% nonbuffered formalin (NFB) and fixed for 24 hr. For transcriptomic analysis, collected hearts were placed in TRIzol for further RNA extraction.

SARS-CoV-2 live virus infection

The immunocardiac co-culture containing hPSC-derived CMs and macrophages were infected with SARS-CoV-2 at an MOI of 0.1 and incubated at 37°C for 24 hr. Infected cells were either lysed in TRIzol for RNA analysis or fixed in 5% formaldehyde for 24 hr for immunofluorescence staining, prior to safe removal from the BSL-3 facility.

hPSC-derived cardiomyocyte differentiation

To differentiate cardiomyocytes (CMs) from hPSC, hPSCs were passaged at a density of 3×10^5 cells/well of 6-well plate and grown for 48 hr in a humidified incubator with 5% CO₂ at 37°C to reach 90% confluence. On day 0, the medium was replaced with RPMI 1640 supplemented with B27 minus insulin and 6 µM CHIR99021. On day 2, the medium was changed to RPMI 1640 supplemented with B27 minus insulin for 24 hr. Day 3, medium was refreshed to RPMI 1640 supplemented with B27 minus insulin and 5 µM XAV939 for 48 h. On day 5, the medium was changed back to RPMI-B27 minus insulin for 48 hr, and then switched to RPMI 1640 plus normal B27 until day 12. The medium was changed every other day. On day 12, the medium was transiently

changed to RPMI 1640 without D-glucose containing ascorbic acid, human albumin and DL-Lactate for two days to allow metabolic purification of CMs. From that day on, fresh RPMI 1640 plus normal B27 was changed every two days. On day 21, cells were dissociated with Accutase at 37°C followed by resuspending with fresh RPMI 1640-B27 plus Y-27632 and reseeding into new plates. After 24 hr, medium was switched to RPMI 1640 plus normal B27 without Y-27632 for following experiments. CMs were derived from two hPSC cell lines: H9-MYH6:mCherry ESCs and WT-F5 iPSCs. The protocol details are summarized in Supplemental Figure 2a.

Adult human cardiomyocytes

Adult human cardiomyocytes were purchased from PromoCell (Primary Human Cardiac Myocytes, C-12810) and cultured in Myocyte Growth Medium (PromoCell, C-22070). Cells were incubated at 37°C with 5% CO₂.

hPSC-derived monocytes and macrophage differentiation

Monocytes and macrophages were derived from two hPSC lines: H9 ESCs and H1 ESCs. The differentiation protocol was adapted from a previously reported protocol (Cao et al., 2019). First, hPSC cells were lifted with ReLeSR (STEMCELL Technologies) as small clusters onto Matrigel-coated 6-well plates at a low density. After 1 day, medium was refreshed with IF9S medium supplemented with 50 ng/ml BMP-4, 15 ng/ml Activin A and 1.5 μM CHIR99021. On day 2, medium was refreshed with IF9S medium supplemented with 50 ng/ml VEGF, 50 ng/ml bFGF, 50 ng/ml SCF (R&D Systems) and 10 μM SB431542 (Cayman Chemical). On day 5 and day 7, medium was changed into IF9S supplemented with 50 ng/ml IL-6 (R&D Systems), 12 ng/ml IL-3 (R&D Systems), 50 ng/ml VEGF, 50 ng/ml bFGF, 50 ng/ml SCF and 50 ng/ml TPO (R&D Systems). On day 9, cells were dissociated with TrypLE (Life Technologies) and resuspended in IF9S medium supplemented with 50 ng/ml IL-6, 12 ng/ml IL-3 and 80 ng/ml M-CSF (R&D Systems) into low attachment plates. On day 13 and day 15, medium was changed into IF9S supplemented with 50 ng/ml IL-6, 12 ng/ml IL-3 and 80 ng/ml M-CSF. Monocytes could be collected on day 15. For macrophage differentiation, monocytes were plated onto FBS-coated plates with IF9S medium supplemented with 80 ng/ml M-CSF. All differentiation steps were cultured under normoxic conditions at 37 °C, 5% CO₂. The protocol details are summarized in Supplemental Fig. 4A.

Monocyte migration assay

The migration of macrophages was examined using 24 well Trans-well chambers (6.5 mm insert; 3.0 μm polycarbonate membrane). The upper well was coated with Matrigel before seeding with macrophages (2X10⁴ cells). After 24 hr, the chamber was fixed and stained with crystal violet. Migrated cells were counted under an inverted light microscope.

Immunocardiac co-culture

hPSC-derived cardiomyocytes were dissociated with Accutase for 5-10 min at 37°C followed by resuspending with fresh RPMI 1640 plus normal B27 and Y-27632 and reseeding into plates. After 24 hr recovery, the medium was switched to RPMI 1640 plus B27 without Y-27632. After another 24 hr recovery, hPSC-derived macrophages were dissociated with Accutase for 3 min and added into hPSC-derived cardiomyocytes. The immunocardiac co-culture cells were cultured for another 24 hr (short-term co-culture) or 7 days (long-term co-culture) before following analysis. Adult

cardiomyocytes were also seeded into plates for 48-96 hr and co-cultured with hPSC-derived macrophages for another 24 hr before following analysis.

SARS-CoV-2 pseudovirus virus infection

To perform pseudovirus infections, cells were seeded into 96 well plates. Spike pseudotyped virus (Han et al., 2021) was added at the indicated MOI=0.01. At 2 hpi, infection media was replaced with fresh media. At 24 hpi, cells were harvested and luciferase activity was measured using the Luciferase Assay System protocol (E1501, Promega) or immunostaining analysis.

Immunostaining

Hamster heart tissues were obtained from mock or SARS-CoV-2 infected hamsters. Heart tissues were fixed overnight in 5% formaldehyde, soaked in 30% sucrose and embedded in OCT (Fisher Scientific, Pittsburgh, PA). The slices were wash with PBS 2 times to remove OCT and incubated in 0.1% Triton for 1hr at room temperature. Then, slices were stained with primary antibodies at 4°C overnight and secondary antibodies at RT for 1 hr. The information for primary antibodies and secondary antibodies is provided in Table S1. Nuclei were counterstained by DAPI.

qRT-PCR

Total RNA samples were prepared from tissues or cells using TRIzol and Direct-zol RNA Miniprep Plus kit (Zymo Research) according to the manufacturer's instructions. To quantify viral replication, measured by the expression of sgRNA transcription of the viral N gene, one-step quantitative real-time PCR was performed using SuperScript III Platinum SYBR Green One-Step qRT-PCR Kit (Invitrogen) with primers specific for the TRS-L and TRS-B sites of the *N* gene as well as *ACTB* or *CTNT* as an internal reference. Quantitative real-time PCR reactions were performed on a LightCycler 480 Instrument II (Roche). Delta-delta-cycle threshold ($\Delta\Delta CT$) was determined relative to the *ACTB* or *CTNT* and mock infected /treated samples. Error bars indicate the standard deviation of the mean from three biological replicates. The sequences of primers/probes are provided in Table S2.

ELISA

CCL2 levels in the supernatant of infected hPSC-derived CMs were evaluated using ELISA. The antibody and cytokine standards were purchased as antibody pairs from R&D Systems (Minneapolis, Minnesota) or Peprotech (Rocky Hill, New Jersey). Individual magnetic Luminex bead sets (Luminex Corp, CA) were coupled to cytokine-specific capture antibodies according to the manufacturer's recommendations. The assays were read on a MAGPIX platform. The median fluorescence intensity of these beads was recorded for each bead and was used for analysis using a custom R script and a 5P regression algorithm.

Sequencing and gene expression UMI counts matrix generation

The 10X libraries were sequenced on the Illumina NovaSeq6000 sequencer with pair-end reads (28 bp for read 1 and 91 bp for read 2). The sequencing data were primarily analyzed by the 10X cellranger pipeline (v3.0.2) in two steps. In the first step, cellranger *mkfastq* demultiplexed samples and generated fastq files; and in the second step, cellranger count aligned fastq files to the reference genome and extracted gene expression UMI counts matrix. In order to measure viral gene expression, we built a custom reference genome by integrating the four virus genes, luciferase and two

fluorescence genes into the 10X pre-built human reference (GRCh38 v3.0.0) using cellranger *mkref*. The sequences of four viral genes (VSV-N, VSV-NS, VSV-M and VSV-L) were retrieved from NCBI (<https://www.ncbi.nlm.nih.gov/nuccore/335873>), the sequence of the luciferase was retrieved from HIV-Luc, and the sequences of the two fluorescence genes were downloaded from NCBI (mCherry: <https://www.ncbi.nlm.nih.gov/nuccore/AY678264.1>; GFP: <https://www.ncbi.nlm.nih.gov/nuccore/U55761.1>).

Single-cell RNA-seq data analysis

We filtered out a small fraction of cells with viral gene content greater than 80% but less than 200 genes detected for which we believe are not real cells but rather empty beads with ambient RNAs. We then filtered out cells with less than 400 or more than 7000 genes detected as well as cells with mitochondria gene content greater than 15%, and used the remaining cells (1654 cells for CM; 1555 cells for CM+virus; 4001 cells for CM+macrophage+virus) for downstream analysis. We normalized the gene expression UMI counts using a deconvolution strategy implemented by the R *scran* package (v.1.14.1). In particular, we pre-clustered cells using the *quickCluster* function; we computed size factor per cell within each cluster and rescaled the size factors by normalization between clusters using the *computeSumFactors* function; and we normalized the UMI counts per cell by the size factors and took a logarithm transform using the *normalize* function. We further normalized the UMI counts across samples using the *multiBatchNorm* function in the R *batchelor* package (v1.2.1). We identified highly variable genes using the *FindVariableFeatures* function in the R *Seurat* package (v3.1.0) (Stuart et al., 2019), and selected the top 3000 variable genes after excluding mitochondria genes, ribosomal genes, dissociation-related genes, viral genes and fluorescence genes. The list of dissociation-related genes was originally built on mouse data (van den Brink et al., 2017); we converted them to human ortholog genes using Ensembl BioMart. We aligned the two samples based on their mutual nearest neighbors (MNNs) using the *fastMNN* function in the R *batchelor* package, this was done by performing a principal component analysis (PCA) on the highly variable genes and then correcting the principal components (PCs) according to their MNNs. We selected the corrected top 50 PCs for downstream visualization and clustering analysis. We ran UMAP dimensional reduction using the *RunUMAP* function in the R *Seurat* package with the number of neighboring points setting to 35 and training epochs setting to 2000. We clustered cells into fifteen clusters by constructing a shared nearest neighbor graph and then grouping cells of similar transcriptome profiles using the *FindNeighbors* function and *FindClusters* function (resolution set to 0.7) in the R *Seurat* package. We identified marker genes for each cluster by performing differential expression analysis between cells inside and outside that cluster using the *FindMarkers* function in the R *Seurat* package. After reviewing the clusters, we merged them into four clusters representing macrophages, CM, CM+macrophages and progenitor cells, for further analysis. We re-identified marker genes for the merged four clusters and selected top 10 positive marker genes per cluster for heatmap plot using the *DoHeatmap* function in the R *Seurat* package. The rest plots were generated using the R *ggplot2* package.

RNA-Seq

Total RNA was extracted in TRIzol (Invitrogen) and DNase I treated using the Directzol RNA Miniprep kit (Zymo Research) according to the manufacturer's instructions. RNA from hamster hearts was homogenized in TRIzol before RNA extraction. RNA-seq libraries of polyadenylated RNA were prepared using TruSeq

Stranded mRNA Library Prep Kit (Illumina) according to the manufacturer's instructions. cDNA libraries were sequenced on an Illumina NextSeq 500 platform. The sequencing reads were cleaned by trimming adapter sequences and low quality bases using cutadapt v1.9.1 (Kechin et al., 2017), and were aligned to the human reference genome (GRCh37) or the SARS-CoV-2 genome (NC_045512.2) using STAR v2.5.2b (Dobin et al., 2013). Sequencing reads from hamster samples were aligned to a hamster reference genome (downloaded from Ensembl, accession#: GCA_000349665) using HISAT2 2.1.0. Raw gene counts were quantified using HTSeq-count v0.11.2 (Anders et al., 2015). Differential expression analysis was performed using DESeq2 v1.22.2 (Love et al., 2014). Regularized log transformation was applied to convert count data to log₂ scale. Sample-to-sample distance matrix was calculated based on the transformed log-scaled count data using R *dist* function. Multidimensional scaling (MDS) was performed on the distance matrix using R *cmdscale* function. PCA plot was drawn using R functions *prcomp*.

Intracellular flow cytometry analysis

Flow cytometry staining was performed to examine the expression of CD14 and CD11B. Briefly, cells were dissociated with Accutase, then washed twice with PBS containing 0.5% BSA and 2mM EDTA. Incubation with antibody was at 4°C for 1 hr in the dark, following by washing twice and flow cytometry analysis. The information for primary antibodies and secondary antibodies is provided in Table S1.

Human studies

For RNA analysis, tissues were acquired by autopsies from deceased COVID-19 human subjects and processed using TRIzol. Tissue samples were provided by the Weill Cornell Medicine Department of Pathology. The uninfected human heart samples were similarly obtained from non-COVID-19 donors. The Tissue Procurement Facility operates under Institutional Review Board (IRB) approved protocol and follows guidelines set by HIPAA. Experiments using samples from human subjects were conducted in accordance with local regulations and with the approval of the institutional review board at the Weill Cornell Medicine under protocol 20-04021814.

Quantification and Statistical analysis

N=3 independent biological replicates were used for all experiments unless otherwise indicated. n.s. indicates a non-significant difference. *P*-values were calculated by unpaired two-tailed Student's t-test unless otherwise indicated. **p*<0.05, ***p*<0.01 and ****p*<0.001.

Reference

- Anders, S., Pyl, P.T., and Huber, W. (2015). HTSeq--a Python framework to work with high-throughput sequencing data. *Bioinformatics* *31*, 166-169. 10.1093/bioinformatics/btu638.
- Blanco-Melo, D., Nilsson-Payant, B.E., Liu, W.C., Uhl, S., Hoagland, D., Moller, R., Jordan, T.X., Oishi, K., Panis, M., Sachs, D., et al. (2020). Imbalanced Host Response to SARS-CoV-2 Drives Development of COVID-19. *Cell*. 10.1016/j.cell.2020.04.026.
- Cao, X., Yakala, G.K., van den Hil, F.E., Cochrane, A., Mummery, C.L., and Orlova, V.V. (2019). Differentiation and Functional Comparison of Monocytes and Macrophages from hiPSCs with Peripheral Blood Derivatives. *Stem Cell Reports* *12*, 1282-1297. 10.1016/j.stemcr.2019.05.003.
- Dobin, A., Davis, C.A., Schlesinger, F., Drenkow, J., Zaleski, C., Jha, S., Batut, P., Chaisson, M., and Gingeras, T.R. (2013). STAR: ultrafast universal RNA-seq aligner. *Bioinformatics* *29*, 15-21. 10.1093/bioinformatics/bts635.
- Han, Y., Duan, X., Yang, L., Nilsson-Payant, B.E., Wang, P., Duan, F., Tang, X., Yaron, T.M., Zhang, T., Uhl, S., et al. (2021). Identification of SARS-CoV-2 inhibitors using lung and colonic organoids. *Nature* *589*, 270-275. 10.1038/s41586-020-2901-9.
- Kechin, A., Boyarskikh, U., Kel, A., and Filipenko, M. (2017). cutPrimers: A New Tool for Accurate Cutting of Primers from Reads of Targeted Next Generation Sequencing. *J Comput Biol* *24*, 1138-1143. 10.1089/cmb.2017.0096.
- Love, M.I., Huber, W., and Anders, S. (2014). Moderated estimation of fold change and dispersion for RNA-seq data with DESeq2. *Genome Biol* *15*, 550. 10.1186/s13059-014-0550-8.
- Stuart, T., Butler, A., Hoffman, P., Hafemeister, C., Papalexi, E., Mauck, W.M., 3rd, Hao, Y., Stoeckius, M., Smibert, P., and Satija, R. (2019). Comprehensive Integration of Single-Cell Data. *Cell* *177*, 1888-1902 e1821. 10.1016/j.cell.2019.05.031.
- van den Brink, S.C., Sage, F., Vertesy, A., Spanjaard, B., Peterson-Maduro, J., Baron, C.S., Robin, C., and van Oudenaarden, A. (2017). Single-cell sequencing reveals dissociation-induced gene expression in tissue subpopulations. *Nat Methods* *14*, 935-936. 10.1038/nmeth.4437.